Optics Letters

High peak and average power Ti:sapphire thin disk amplifier with extraction during pumping

Vladimir Chvykov,[1,*] Huabao Cao,[1] Roland Nagymihaly,[1] Mikhail P. Kalashnikov,[1,2] Nikita Khodakovskiy,[2] Richard Glassock,[1] Lutz Ehrentraut,[2] Matthias Schnuerer,[2] and Károly Osvay[1]

[1]ELI-HU Non-Profit Ltd., Dugonics tér 13, H-6720 Szeged, Hungary
[2]Max Born Institute for Nonlinear Optics and Short Pulse Spectroscopy, Max-Born-Strasse 2a, 12489 Berlin, Germany
*Corresponding author: Vladimir.Chvykov@eli-alps.hu

Received 17 May 2016; accepted 26 May 2016; posted 27 May 2016 (Doc. ID 265058); published 24 June 2016

The combination of the extraction during pumping (EDP) amplification scheme and the thin disk (TD) technology has been successfully applied to the Ti:sapphire (Ti:sa) laser medium for the first time, to the best of our knowledge. In a proof-of-principle experiment, we demonstrate high energy broadband amplification in a room temperature water cooled EDP-TD head of stretched femtosecond pulses at a 10 Hz repetition rate, instead of performing a cryogenically cooled traditional multi-pass scheme. Hence, the EDP-TD combination can overcome the limits associated with thermal effects and transverse amplified spontaneous emission, enabling Ti:sa laser systems to have a petawatt peak and hundreds of watts of average power.

OCIS codes: (140.7090) Ultrafast lasers; (140.3590) Lasers, titanium; (140.3280) Laser amplifiers.

http://dx.doi.org/10.1364/OL.41.003017

Present day chirped pulse amplification (CPA) [1,2] laser systems have reached a few petawatts (PW) of peak power [3], and the roadmaps are scheduled to perform at 10–100 PW in the near future [4,5]. This breakthrough of the one PW regime has become possible due to the application of large aperture Ti:sapphire (Ti:sa) crystals in the final amplifiers in conjunction with the extraction during pumping (EDP) technique for efficient energy extraction [3,6–9], and is one of the most promising ways to reach the next milestone. Such systems could be widely applied to many areas of science and industry as the sources of TeV electron beams, GeV ion beams [10], and as secondary sources for ultra-bright x and γ rays [11]. However, the wide application of these sources will be strongly limited unless the repetition rate of laser systems reach the tens of hertz (Hz) to sub-kilohertz (kHz) regime, but in this case, the gain medium endures significant, and often detrimental, thermal loading.

The thin disk (TD) laser technology that has been intensively developed during the last decade for high average power lasers has demonstrated an ability to overcome thermal distortions and damages of laser crystals [12–14] by the extraction of heat from the whole aperture of the active medium. This allows for a more effective and spatially uniform heat removal due to the significantly larger cooling surface compared to the conventional side-surface heat extraction.

TD technology may offer the potential to be used in systems with both high peak and average output power too. So far, research and development have been mainly devoted to a relatively narrow emission spectral band media (doped YAGs), and hence, the pulse duration is limited to a picosecond (ps) range. The application of this technology to Ti:sa laser materials may allow the combination of broadband pulse amplification at a kilowatt (kW) average power. In this configuration, on one hand, the suppression of the transverse amplified spontaneous emission (TASE) and the transverse parasitic generation (TPG) are the primary challenges (EDP [7–9]). On the other hand, the low gain and low pump absorption of the TD amplifiers complicate its scheme and leads to multi-passing for both the pump and seed. A medium with a large emission cross section and a high concentration of active ions, such as Ti:sa, can help to overcome this problem too.

It was recently suggested that a combination of the TD amplification with the EDP method maintains the broad bandwidth and minimizes energy losses associated with TASE in thin crystals, while overcoming the thermal effects associated with the high repetition rate. Numerical simulations related to the EDP-TD Ti:sa amplifiers were performed for different amplifier geometries and parameters of the amplification, and based on the computation modeling, optimized designs of a 0.1–10 PW Ti:sa EDP-TD power amplifier with tens of Hz-kHz repetition rates as well as the thermal dynamic behavior were predicted [15].

In this Letter, we present a proof-of-principle experiment of the operation of a broadband EDP-TD amplifier in a 100 TW CPA laser system. The amplifier head is fully characterized, including the measurement and modelling of the temperature distribution, dynamics of amplification, and wave front of the amplified pulses.

A commercial amplifier system of a CPA laser in the Max-Born-Institute served as a test bed, providing 100 TW peak power and 28 fs laser pulses at a 10 Hz repetition rate [16]. In the experiment, the final cryogenically cooled Ti:sa amplifier

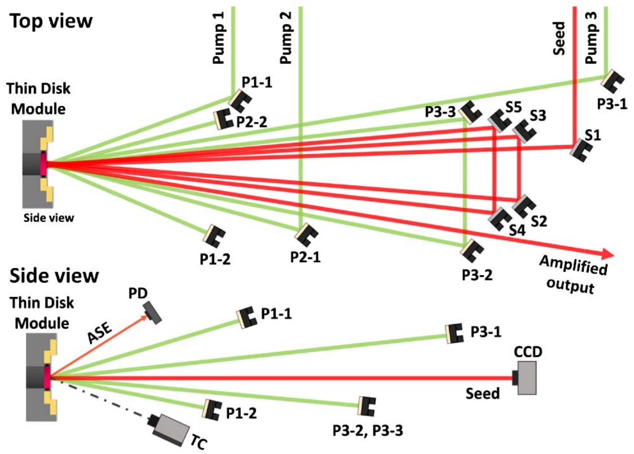

Fig. 1. Schematic diagram of the experimental setup. The green beams are the pump; the red beams are seed passes. Mirrors P1-1 and P1-2 were used for pump laser 1, mirrors P2-1 and P2-2 were used for pump 2, mirrors P3-1, P3-2, and P3-3 were used for pump 3. The layout of the seed amplification consists of mirrors S1–S5. The incidence angles are exaggerated for clarity.

has been replaced with the EDP-TD room temperature cooled arrangement (Fig. 1). The Ti:sa crystal with a 35 mm diameter, 3 mm thickness, and an absorption coefficient of 2 cm^{-1} was mounted in the homemade TD head module. The amplifier was designed in the scheme of an active mirror. The front surface of the crystal was anti-reflectance (AR) coated, while the rear side was high-reflectance (HR) coated for both pump (532 nm) and seed (800 nm) wavelengths. The absorbing material IR140 (Exciton, refraction index of 1.76 at 800 nm), dissolved in a series M liquid (Cargill Labs), was applied to the surface sides of the Ti:sa crystal for TASE and TPG suppression. The rear surface of the crystal was actively water cooled to room temperature. An area of 24 mm diameter was pumped by three electronically synchronized lasers, each providing a 15 ns, 2 J pulse at a 532 nm wavelength.

Each of the three pump beams passed through the TD twice. One pass includes the reflection from the rear surface of the crystal, effectively resulting in four passes per pump beam. The total absorption for the double pass of the pump was measured to be 85%. Mirrors P1-1 and P1-2 were used for directing the pump laser 1 to the Ti:sa crystal, mirrors P2-1 and P2-2 were used for pump 2, and mirrors P3-1, P3-2, and P3-3 were used for pump 3. In contrast to pump 3, the double passing of pump 1 and pump 2 was realized by the retro-reflection of P1-2 and P2-2, respectively. The P1-2 and P2-2 mirrors were slightly tilted to prevent damage to the pump lasers from residual reflected pump beams. The side view demonstrates the vertically separated pump beams with the smallest incidence angles, where pump 2 was omitted. A positively stretched seed (0.5 J energy, pulse duration of few hundred ps) was amplified during three passes (mirrors S1–S5) with a total gain of about five.

Despite the use of the liquid absorber, severe parasitic lasing was generated in the absence of the seed when the active medium was simultaneously pumped with the double passed pump beams 1 and 3 with total absorbed energy of about 3.4 J. This is clearly visible on the oscillogram of the luminescence

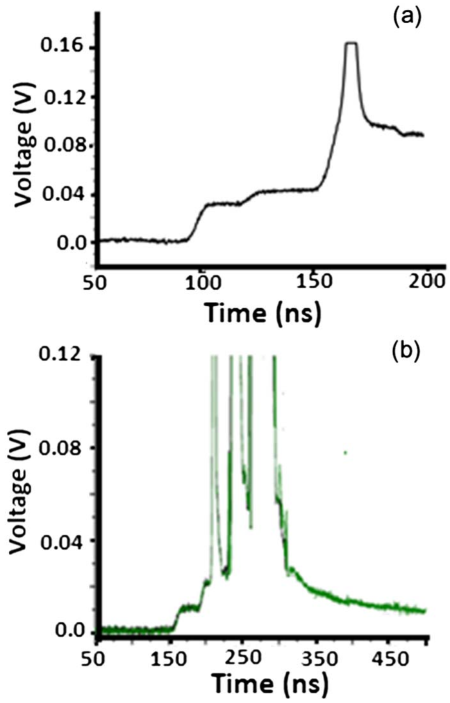

Fig. 2. Oscillogram of the luminescence from the Ti:sa crystal. (a) Parasitic generation after the double pass of pump beams 1 and 3 with total absorbed energy about 3.4 J. (b) The luminescence with three seed passes.

from the Ti:sa crystal shown in Fig. 2(a). To avoid TPG losses, the EDP technique was applied, extracting energy from the crystal before the second pass of pump 3 (~3 J of absorbed energy).

The second pass of pump 3 was delayed about 20 ns from first one and added 0.4 J to the stored energy after the extraction of 0.5 J by the first seed pass (total amplified energy after the first pass was about 1 J). The pump pulse from pump laser 2 was added between the second and third seed passes [Fig. 2(b)], which avoided another round of parasitic generation, reaching 2.6 J of the amplified energy when the total absorbed pump was about 5 J.

This seed amplification was achieved by only three passes and two passes of the pump (compared with the tens of passes of the conventional Nd:YAG or Yb:YAG TD amplifiers) due to the much greater emission cross section and doping of the Ti:sa crystal. Figure 3 shows the typical near field cross section of the (a) flat-top pump and (b) seed amplified after the third pass beams. The deviation from the flat-top energy distribution

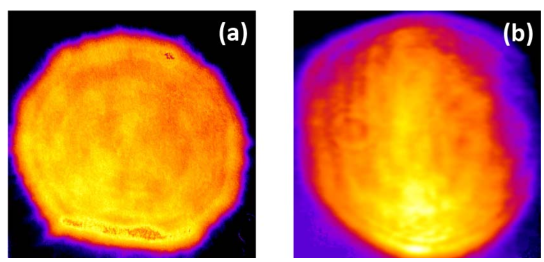

Fig. 3. Near field cross section of (a) the typical pump beam and (b) the seed beam after the third pass.

of the seed beam is induced by the slightly cylindrical rear surface of the used Ti:sa crystal, and is due to a manufacturing defect.

The temperature distribution over the crystal input surface in the transverse direction through the crystal was measured (Fig. 4) with a thermal imager (TIM-160, Micro-Epsilon). The recordings were made during pumping of the crystal with 4 J of pulse energy at a 10 Hz repetition rate without the energy extraction by the seed. The initial temperature of the coolant was 18°C with an average flow speed of about 7 cm^3/s.

The crystal mounted in the holder in Fig. 4 (inset) looks asymmetrical due to the thermal imager location below it (see Fig. 1). Nevertheless, this parallax did not affect the measurement of the temperature of the horizontal transverse distribution of the mean section through the crystal in the pump area (red curve in Fig. 4). Figure 5 shows the temperature growth dynamic taken at the central point of the crystal until the temperature stabilization; that is, after the heating stabilization, during the crystal pumping within 20 s with 10 Hz repetition rate of the pump pulses.

Figures 4 and 5 show that a coolant temperature of 18°C was sufficient to keep the maximal crystal temperature after stabilization under 30°C. The variation through the pump area was only 3°C, which does not significantly affect the seed beam wave front, and will be shown later. We propose that most of the pump energy was transmitted to the crystal heating due to TASE absorption by the liquid absorber, which is the largest portion of total luminescence. That means that the similar maximum temperature and its distribution could be seen with the crystal being pumped at the same repetition rate, with 8 J per pump pulse with half of this energy being extracted by the seed.

Furthermore, this result could be improved significantly using a chiller with a higher coolant flow speed. Figure 5 shows that the flow rate was too slow in these experiments; after the pumping was stopped, 5 s was required to cool the crystal to 22°C.

The impact on the beam wave front was also measured during these crystal heating conditions. The expanded beam of a He–Ne laser was used to completely cover the Ti:sa crystal

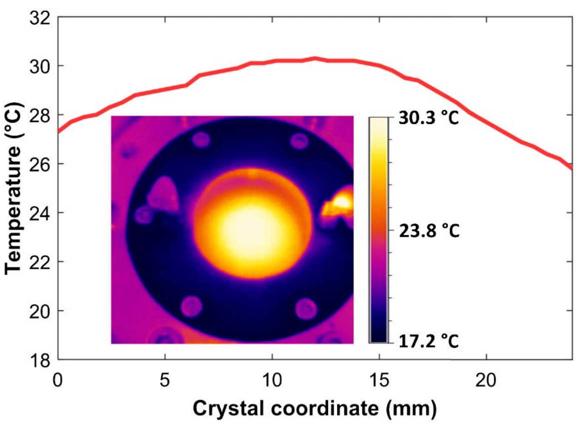

Fig. 4. Temperature distribution through the amplifier crystal after temperature stabilization during pumping by the 4 J per pulse at a 10 Hz repetition rate. The curve shows the temperature distribution of the horizontal mean section of the pumped area (red, solid line) and temperature distribution in the amplifier head (inset).

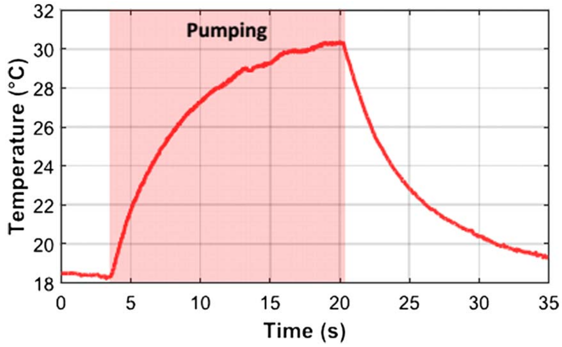

Fig. 5. Temperature growth dynamics of the central point of the Ti:sa crystal.

aperture and, after reflection from the rear surface and diameter reduction by a telescope, was directed to a high-altitude science operation Shack–Hartmann wave front sensors.

Measurements were taken until the crystal temperature was stabilized. Figure 6 shows the two wave front diagrams before heating and after temperature stabilization. The measured wave front parameters before and after pumping are consequently peak to valley (P-V): 0.32 μm; root mean square (RMS): 0.06 μm and after heating stabilization P-V: 1.51 μm; RMS: 0.39 μm. These results are better than the comparable single shot laser systems with a side extraction of the heat measured before the wave front correction [17].

Heat extraction from the Ti:sa TD was numerically modelled using the finite element method (FEM). The method was modified to match experimental conditions and scaling up the system for higher repetition rates. The 3D model consisted of the Ti:sa crystal, with the same parameters as the experimental crystal, and the crystal holder with a rectangular flow channel with dimensions of 3 mm × 50 mm × 90 mm. The gain medium was pumped by 4 J pulses at a 532 nm wavelength and a 10 Hz repetition rate, from which 90% of the energy was absorbed. The maximum thermal load case was calculated with all the absorbed pump energy considered to be dissipated in the crystal as heat; the equivalent to the case of the 8 J pump energy when 50% was extracted by the seed. The coolant flow was modeled in the channel coupled with the heat transfer in full geometry. The experimentally-used average flow velocity was around 0.4 m/s, which indicates that a laminar model could be used. The simulations fit well with the experimental results with a coolant temperature of 18°C.

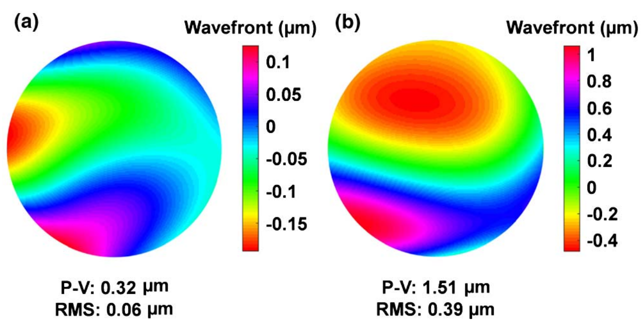

Fig. 6. Wave front profiles (a) before heating and (b) after temperature stabilization.

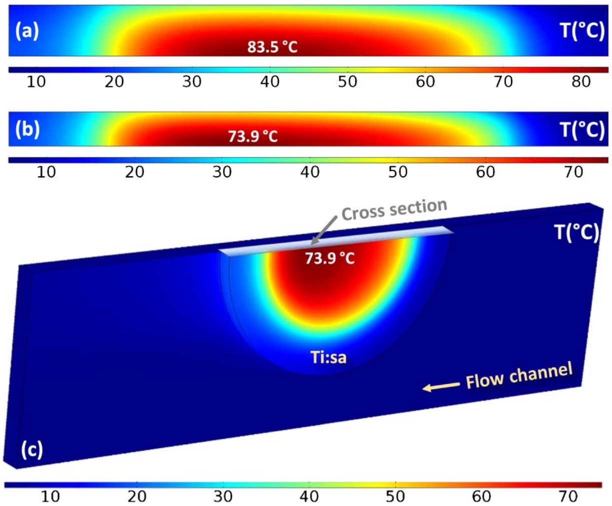

Fig. 7. Plots of the steady-state temperature distribution in the central cross section parallel with the flow direction: (a) 3 mm, (b) 2 mm thick crystals, and (c) the entire modeled domain for a 2 mm thick crystal. The flow velocity was set to 5 m/s in both cases. Only half of the real geometry is visualized as a symmetry boundary condition and was used at the center to optimize the computational costs. Temperature values inside the plots are related to the peak temperature.

The repetition rate in our model was increased to 100 Hz, corresponding to the 360 W of the thermal load, in order to scale of our TD setup for a higher average power. These model parameters account for the 8 J pumping with an energy extraction efficiency by amplification of the seed pulses of 50%. Proper cooling conditions were considered using a flow velocity of 5 m/s, and applied to the low Reynolds-number $k-\epsilon$ turbulent model to account for the higher velocity gradients close to the contact surface. The coolant temperature was decreased to 5°C, the lowest reasonable value for water cooling. For optimization of conditions, 3 and 2 mm thick crystals were used (Fig. 7).

In the case of the 3 mm crystal, two passes for the pump pulses were considered to reach the 90% absorption, one pass includes the input and back reflection from the HR coated rear side of the crystal. For the 2 mm crystal, three passes for the pump were required to reach the same absorption. Figure 7 shows that the temperature profile of the thinner crystal is much more symmetric and smoother than the thick crystal. This improves the temperature difference between the center and the edges with central peak temperatures of 83.5°C and 73.5°C for the 3 and 2 mm thick crystals, respectively.

In conclusion, we have presented the results of a proof-of-principle experiment with an EDP-TD Ti:sa amplifier. The obtained results demonstrate the capacity to build a room temperature cooled final amplifier, providing few Joules of energy of the seed laser pulses with in a 100 s TW/10 s Hz CPA laser system. The EDP-TD amplifier was brought to saturation, reaching the close to theoretical maximum efficiency of ~50% at only three amplification passes. This is a considerable simplification of the amplifier scheme compared to the conventional ten passes TD-amplifiers. Simulations also supported the findings that the new amplifier design overcomes the limitations associated with thermal wave front distortion of the amplified pulse, and losses due to TASE and TPG in high peak and average power laser systems, enabling the scaling up of the system to the repetition rate of hundreds of Hz, or to a PW-level output peak power for tens of Hz repetition rates.

Funding. ELI-ALPS (GINOP 2.3.6-15-2015-00001); LASERLAB-EUROPE (284464, EC-FP7).

Acknowledgment. The authors thank Daniel Papp for the useful ideas in the numerical modeling.

REFERENCES

1. T. Damm, M. Kaschke, F. Noack, and B. Wilhelmi, Opt. Lett. **10**, 176 (1985).
2. D. Strickland and G. Mourou, Opt. Commun. **56**, 219 (1985).
3. Y. Chu, Z. Gan, X. Liang, L. Yu, X. Lu, C. Wang, X. Wang, L. Xu, H. Lu, D. Yin, Y. Leng, R. Li, and Z. Xu, Opt. Lett. **40**, 5011 (2015).
4. H. Cao, X. Lu, and D. Fan, Appl. Opt. **51**, 2150 (2012).
5. www.eli-laser.eu.
6. D. Joyce, B. Ripley, and K. Schid, Laser Focus World **46**, 37 (2010).
7. V. Chvykov, V. Yanovsky, S.-W. Bahk, G. Kalintchenko, and G. Mourou, in *Conference on Lasers and Electro-Optics*, OSA Technical Digest CLEO (2003), paper CWA34.
8. V. Chvykov and K. Krushelnick, Opt. Commun. **285**, 2134 (2012).
9. V. Chvykov, J. Nees, and K. Krushelnick, Opt. Commun. **312**, 216 (2014).
10. G. A. Mourou, N. J. Fisch, V. M. Malkin, Z. Toroker, E. A. Khazanov, A. M. Sergeev, T. Tajima, and B. Le Garrec, Opt. Commun. **285**, 720 (2012).
11. G. Mourou, T. Tajima, and S. Bulanov, Rev. Mod. Phys. **78**, 309 (2006).
12. A. Giesen, Laser Tech. J. **2**, 42 (2005).
13. J. Speiser, J. Opt. Soc. Am. B **26**, 26 (2009).
14. J.-P. Negel, A. Voss, M. A. Ahmed, D. Bauer, D. Sutter, A. Killi, and T. Graf, Opt. Lett. **38**, 5442 (2013).
15. V. Chvykov, R. S. Nagymihaly, H. Cao, M. Kalashnikov, and K. Osvay, Opt. Express **24**, 3721 (2016).
16. www.mbi-berlin.de/en/research/projects/4.2/HFL.
17. S.-W. Bahk, P. Rousseau, T. A. Planchon, V. Chvykov, G. Kalintchenko, A. Maksimchuk, G. A. Mourou, and V. Yanovsky, Opt. Lett. **29**, 2837 (2004).